Supporting Information

CO_2-tolerant (Y, Tb)Ba(Co, Ga)$_4O_7$ Cathodes with Low Thermal Expansion for Solid Oxide Fuel Cells

Ke-Yu Lai and Arumugam Manthiram[*]

Materials Science and Engineering Program and Texas Materials Institute, The University of Texas at Austin, Austin, Texas 78712, United States

*Corresponding Author: rmanth@mail.utexas.edu

Calculation of the average metal-oxygen bond energy

The average metal (R, Ba, and M) – oxygen bond energies (<MOE>) in swedenborgite oxides ($RBaM_4O_7$) were obtained from the average R–O (<R–O>), Ba–O (<Ba–O>), and M–O (<M–O>) bond energies. The following calculation for $R_{1-x}R'_xBa(M_{1-y}M'_y)_4O_7$ was adapted from the average metal-oxygen bond energy calculation in perovskite oxides.[S1]

$$< MOE > = < R - O > + < Ba - O > + 4 < M - O > \quad (S1)$$

$$< R - O > = \Delta(R - O) + \Delta(R' - O) \quad (S2)$$

$$< M - O > = \Delta(M - O) + \Delta(M' - O) \quad (S3)$$

$$\Delta(R - O) = \frac{x_R}{CN_R \cdot m}\left(\Delta H_{R_mO_n} - m \cdot \Delta H_R - \frac{n}{2} D_{O_2}\right) \quad (S4)$$

$$\Delta(M - O) = \frac{x_M}{CN_M \cdot m}\left(\Delta H_{M_mO_n} - m \cdot \Delta H_M - \frac{n}{2} D_{O_2}\right) \quad (S5)$$

In the above equations, x_R and x_M are, respectively, molar fractions of the R and M cations. ΔH_{RmOn} and $\Delta H_{R(M)}$ represent, respectively, the enthalpy of formation of R_mO_n and the

sublimation energy of the R metal, which were obtained from the thermodynamic data and are listed below.

ΔH_{Y2O3} = -1905.3 kJ mol^{-1}, ΔH_{Y} = 421.3 kJ mol^{-1}

ΔH_{Tb2O3} = -1865.2 kJ mol^{-1}, ΔH_{Tb} = 388.7 kJ mol^{-1}

ΔH_{BaO} = -553.5 kJ mol^{-1}, ΔH_{Ba} = 180 kJ mol^{-1}

ΔH_{Co2O3} = -653.1 kJ mol^{-1}, ΔH_{CoO} = -237.9 kJ mol^{-1}, ΔH_{Co} = 424.7 kJ mol^{-1}

ΔH_{Ga2O3} = -1089.1 kJ mol^{-1}, ΔH_{Ga} = 272.0 kJ mol^{-1}

CN is the coordination number of each cation, where CN_R, CN_{Ba}, and CN_M are, respectively, 6, 12, and 4. D_{O2} is the dissociation energy of O_2 (e.g. 500.2 kJ mol^{-1}).

Reference

(S1) Zhu, Y.; Sunarso, J.; Zhou, W.; Shao, Z. Probing CO2 Reaction Mechanisms and Effects on the SrNb0.1Co0.9−xFexO3−δ Cathodes for Solid Oxide Fuel Cells. *Appl. Catal. B Environ.* **2015**, *172–173*, 52–57.

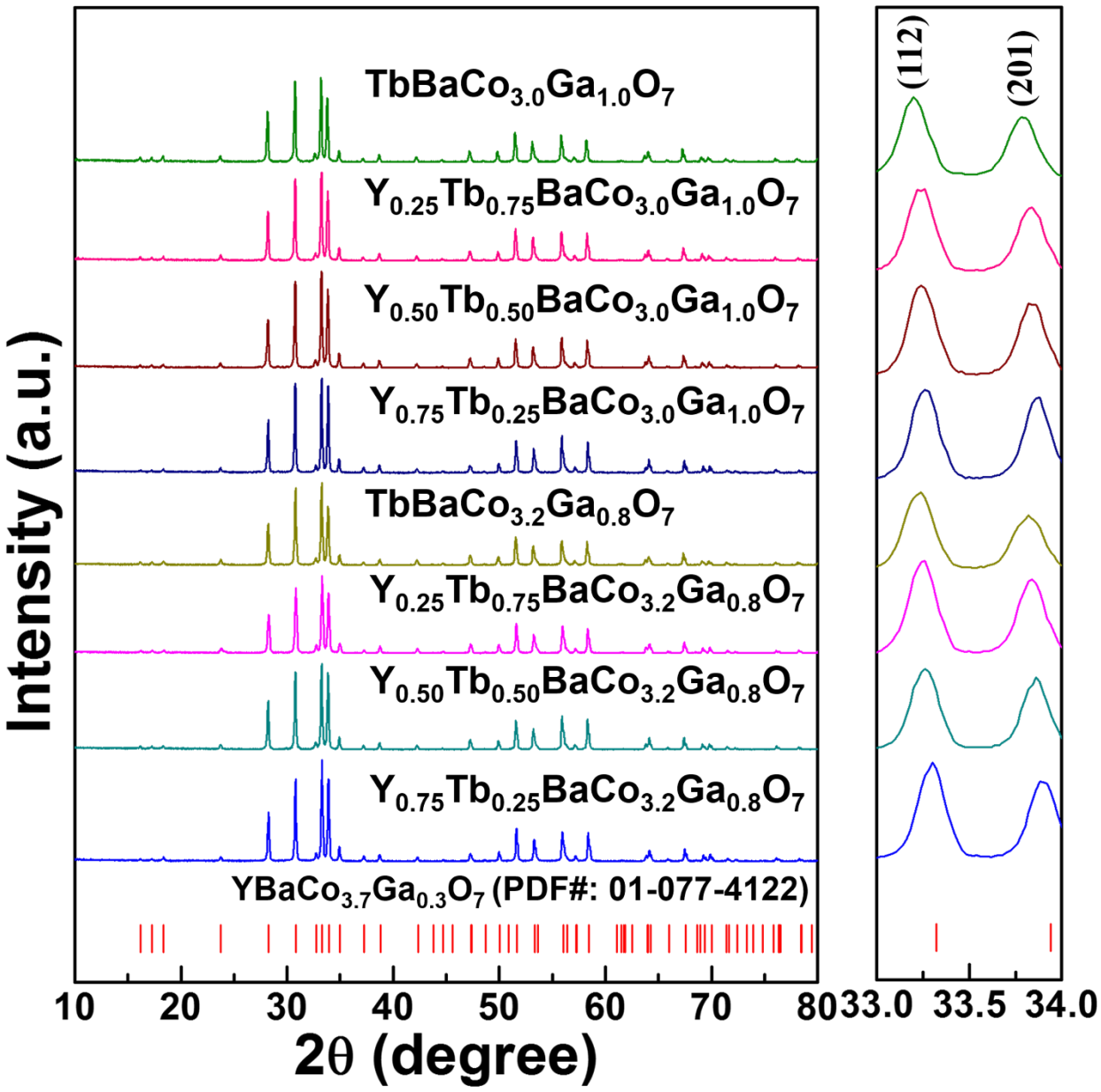

Fig. S1. RT-XRD patterns of the (Y, Tb)Ba(Co, Ga)$_4$O$_{7+\delta}$ powder samples, which were synthesized by a solid-state reaction at 1200 °C for 24 h. The red bars indicate the peak positions of $YBaCo_{3.7}Ga_{0.3}O_7$ with a trigonal structure and P31c space group (PDF#: 01-077-4122).

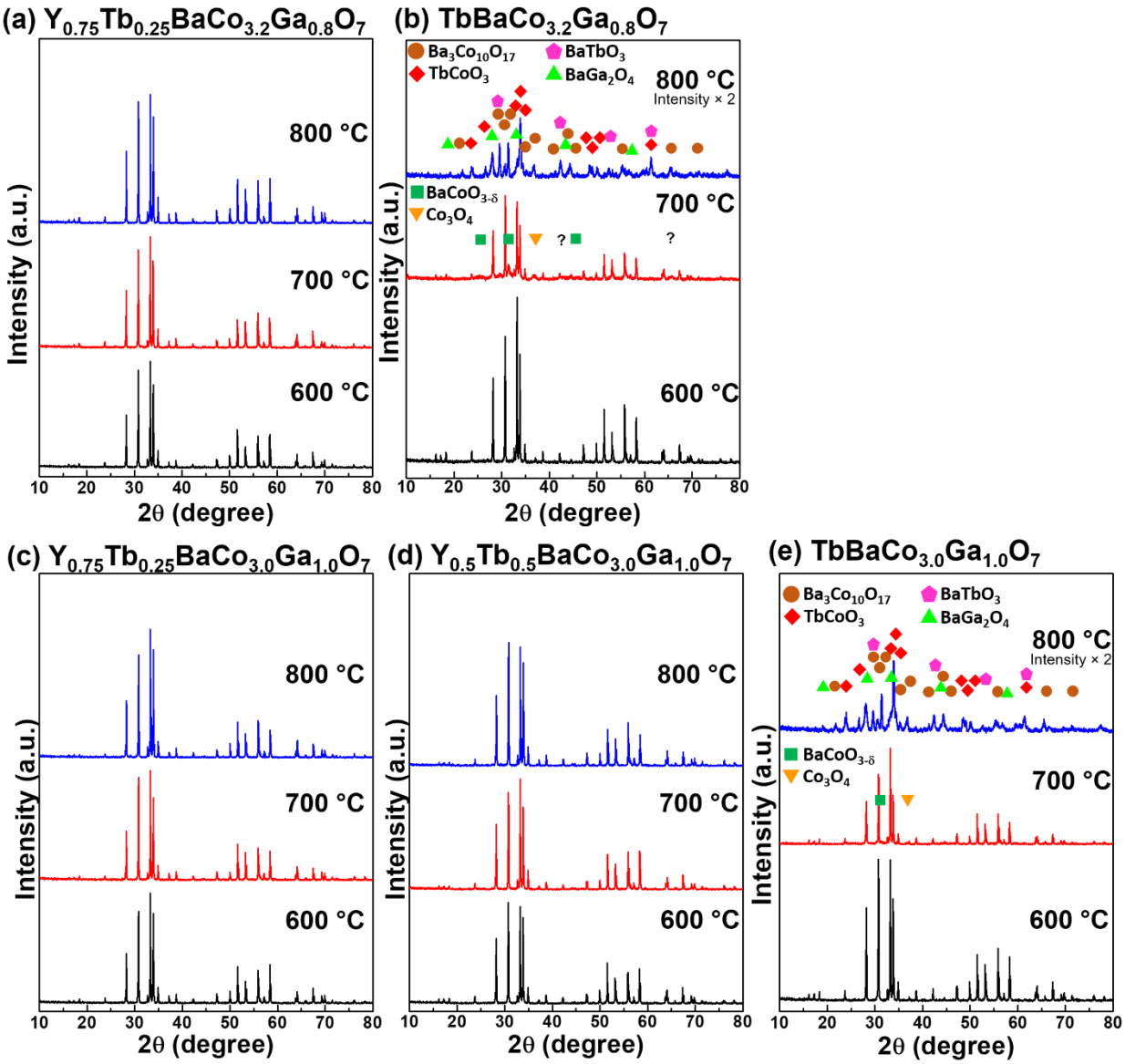

Fig. S2. Room-temperature XRD patterns of the (a) $Y_{0.75}Tb_{0.25}BaCo_{3.2}Ga_{0.8}O_{7+\delta}$, (b) $TbBaCo_{3.2}Ga_{0.8}O_{7+\delta}$, (c) $Y_{0.75}Tb_{0.25}BaCo_{3.0}Ga_{1.0}O_{7+\delta}$, (d) $Y_{0.5}Tb_{0.5}BaCo_{3.0}Ga_{1.0}O_{7+\delta}$, and (e) $TbBaCo_{3.0}Ga_{1.0}O_{7+\delta}$ samples annealed at 600 – 800 °C for 120 h. The swedenborgite phase of $TbBaCo_{3.2}Ga_{0.8}O_{7+\delta}$ and $TbBaCo_{3.0}Ga_{1.0}O_{7+\delta}$ decompose completely at 800 °C, and the XRD pattern intensities of these samples were doubled in order to observe clearly.

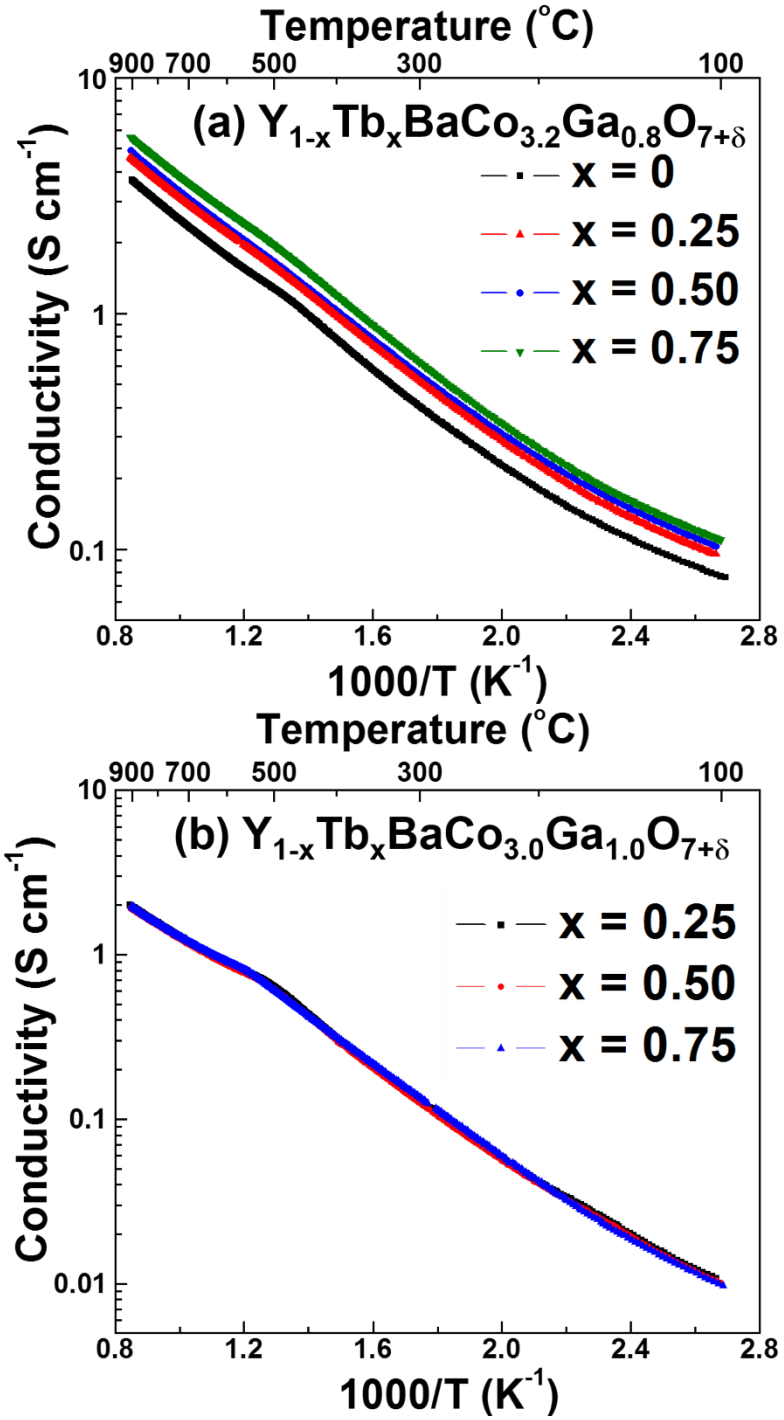

Fig. S3. Electrical conductivity plots of (a) (Y, Tb)$BaCo_{3.2}Ga_{0.8}O_{7+\delta}$ and (b) (Y, Tb)$BaCo_{3.0}Ga_{1.0}O_{7+\delta}$ in air from 100 to 900 °C with a heating rate of 3 °C min^{-1}.

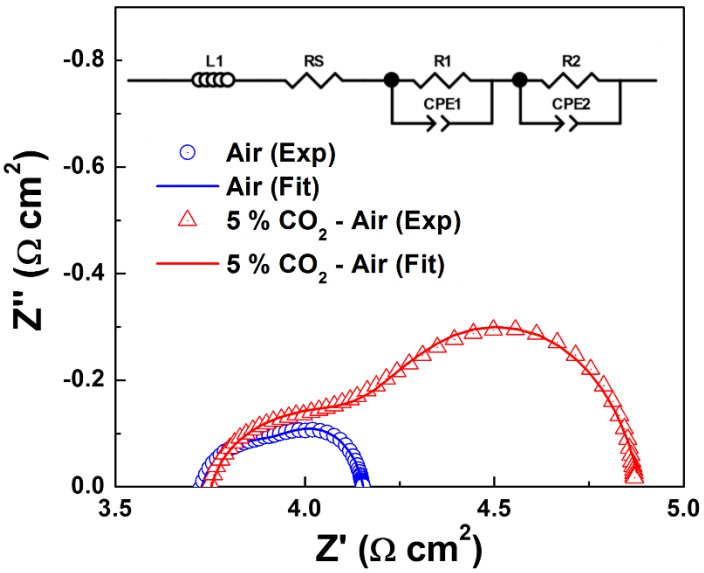

Fig. S4. Nyquist plots of the impedance spectra of $Y_{0.5}Tb_{0.5}BaCo_{3.2}Ga_{0.8}O_{7+\delta}$ – GDC composite cathode at 600 °C in air (the data point at 0 min of Fig. 6a) and 5 % CO_2 – air (the data point at 780 min of Fig. 6a). An equivalent-circuit model with the L1-RS-(R1-CPE1)-(R2-CPE2) configuration was used in the impedance spectrum analysis. L1 is the inductance from the metal leads, and RS is the ohmic resistance of the leads and electrolyte. The constant phase element (CPE) describes the electrochemical reactions on an interface as an imperfect capacitor. High-frequency resistance (R1) generally refers to the charge transfer processes, and low-frequency resistance (R2) includes the non-charge transfer processes of the ORR, such as oxygen adsorption, dissociation, desorption, and mass transport.

Table S1. The fitting parameters of the impedance spectra of the $Y_{0.5}Tb_{0.5}BaCo_{3.2}Ga_{0.8}O_{7+\delta}$ – GDC composite cathode at 600 °C in air (the data point at 0 min of Fig. 6a) and 5 % CO_2 – air (the data point at 780 min of Fig. 6a).

600 °C	Air	5 % CO_2 – Air
L1 (H cm^{-2})	7.8×10^{-7}	6.2×10^{-7}
Rs (Ω cm^2)	3.68	3.71
R1 (Ω cm^2)	2.89×10^{-1}	5.70×10^{-1}
CPE1-Q (F S^{n-1} cm^{-2})	1.71×10^{-2}	2.86×10^{-2}
CPE1-n	0.611	0.532
CPE1-Q_{equ} (F cm^{-2})	5.82×10^{-4}	7.63×10^{-4}
R2 (Ω cm^2)	1.83×10^{-1}	6.20×10^{-1}
CPE2-Q (F S^{n-1} cm^{-2})	3.62×10^{-2}	6.88×10^{-2}
CPE2-n	0.901	0.887
CPE2-Q_{equ} (F cm^{-2})	2.09×10^{-2}	4.60×10^{-2}
χ^2 (goodness of fit)	1.43×10^{-5}	3.54×10^{-5}

The CPE is expressed in terms of pseudo-capacitance Q and model parameter n as in the equation S6 below, where ω is frequency.

$$Z_{CPE} = \frac{1}{(j\omega)^n Q} \quad (S6)$$

The equivalent capacitance CPE-Q_{equ} can be calculated with the following equation S7.[S2]

$$Q_{equ} = R^{(1-n)/n}\, Q^{1/n} \quad (S7)$$

Reference

(S2) Narendar, N.; Mather, G. C.; Dias, P. A. N.; Fagg, D. P. The Importance of Phase Purity in Ni–BaZr0.85Y0.15O3−δ Cermet Anodes – Novel Nitrate-Free Combustion Route and Electrochemical Study. *RSC Adv.* **2012**, *3*, 859–869.

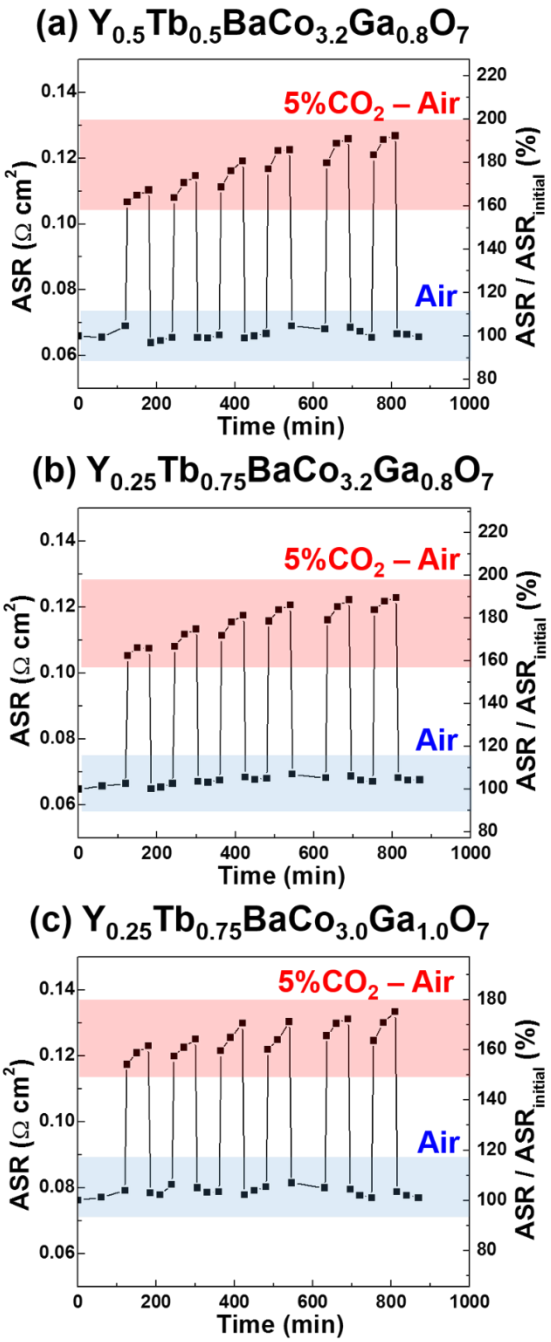

Fig. S5. ASR evolution curves of the (a) $Y_{0.5}Tb_{0.5}BaCo_{3.2}Ga_{0.8}O_{7+\delta}$ – GDC, (b) $Y_{0.25}Tb_{0.75}BaCo_{3.2}Ga_{0.8}O_{7+\delta}$ – GDC, and (c) $Y_{0.25}Tb_{0.75}BaCo_{3.0}Ga_{1.0}O_{7+\delta}$ – GDC composite cathodes during six cycles of gas alternation between 5 % CO_2 – air and pure air at 700 °C. Each gas was purged for 60 min with a flow rate of 100 ml min^{-1}.

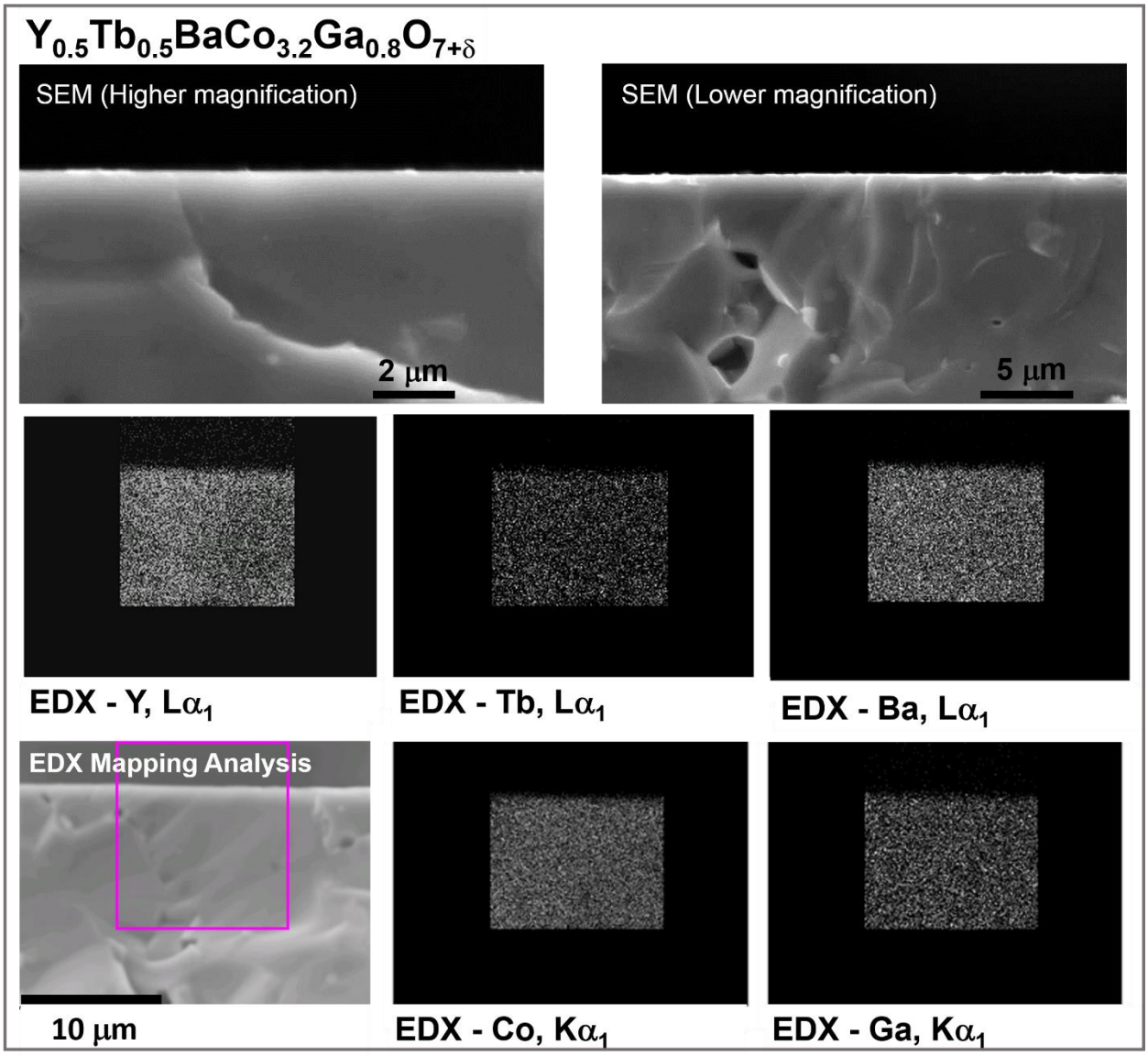

Fig. S6. Cross-sectional SEM images and EDX mapping results of the dense pellet surface of $Y_{0.5}Tb_{0.5}BaCo_{3.2}Ga_{0.8}O_{7+\delta}$ after annealing at 600 °C in 5 % CO_2 – air for 50 h. No obvious $BaCO_3$ layer is found.

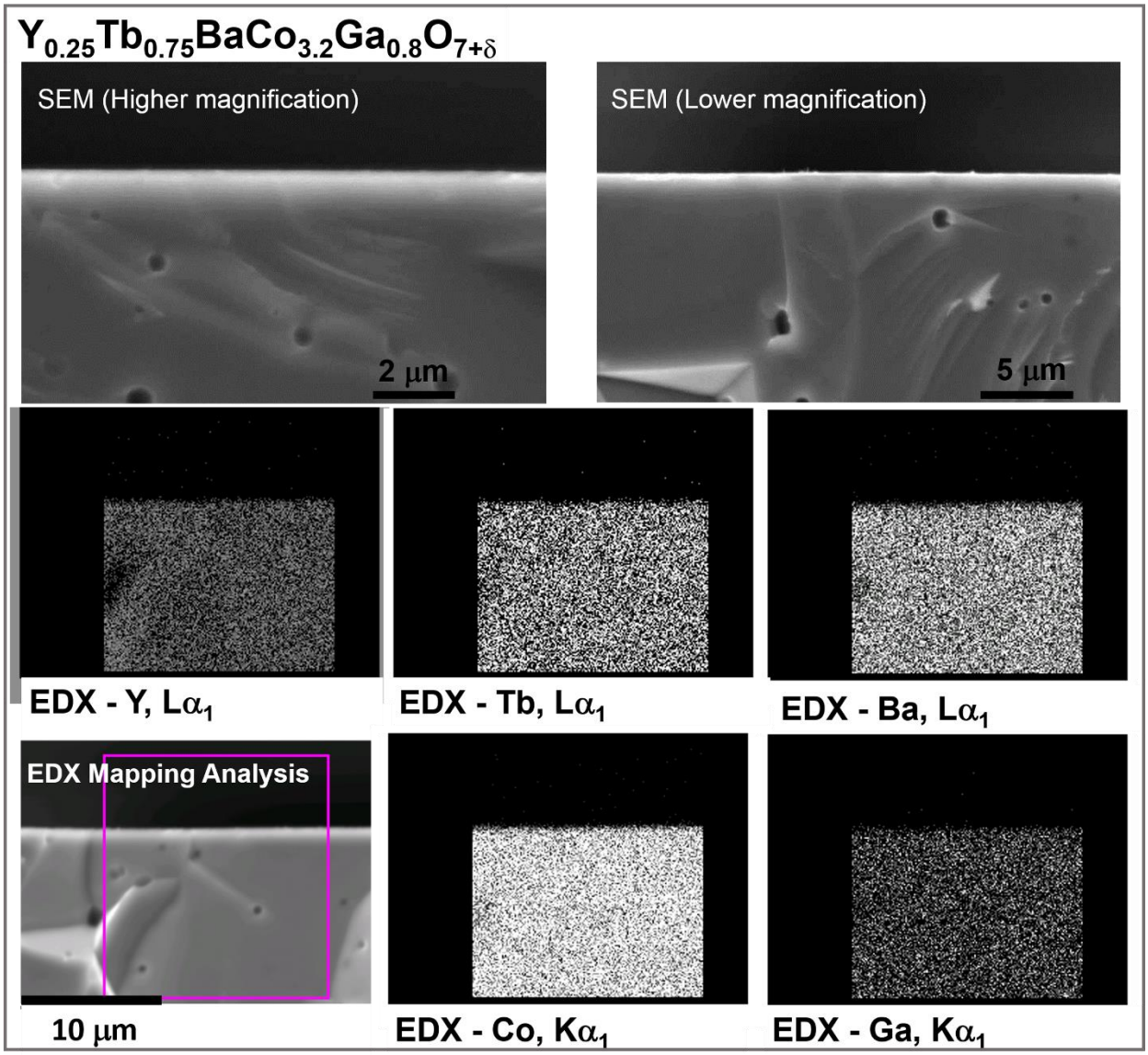

Fig. S7. Cross-sectional SEM images and EDX mapping results of the dense pellet surface of $Y_{0.25}Tb_{0.75}BaCo_{3.2}Ga_{0.8}O_{7+\delta}$ after annealing at 600 °C in 5 % CO_2 – air for 50 h. No obvious $BaCO_3$ layer is found.

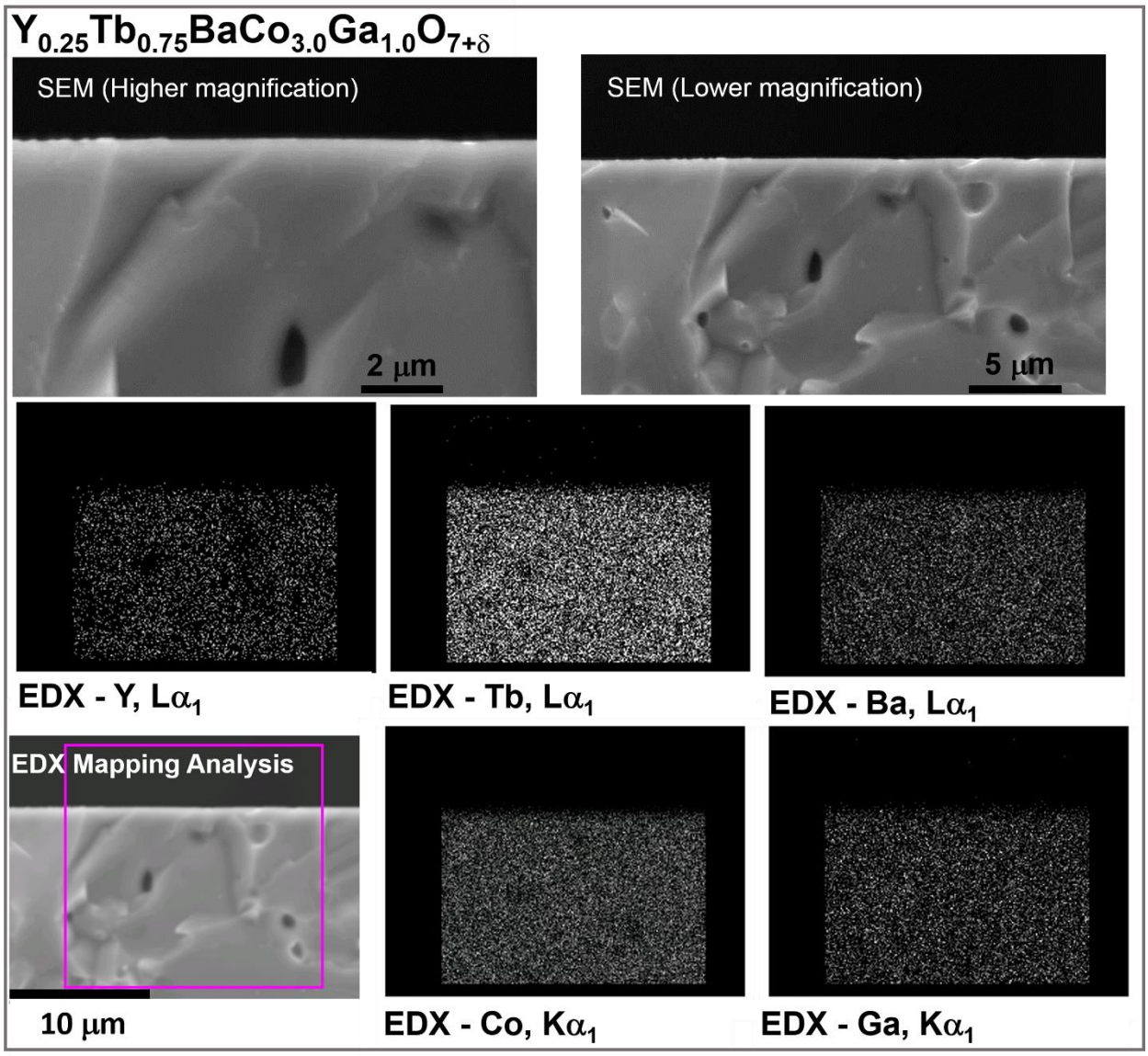

Fig. S8. Cross-sectional SEM images and EDX mapping results of the dense pellet surface of $Y_{0.25}Tb_{0.75}BaCo_{3.0}Ga_{1.0}O_{7+\delta}$ after annealing at 600 °C in 5 % CO_2 – air for 50 h. No obvious $BaCO_3$ layer is found.

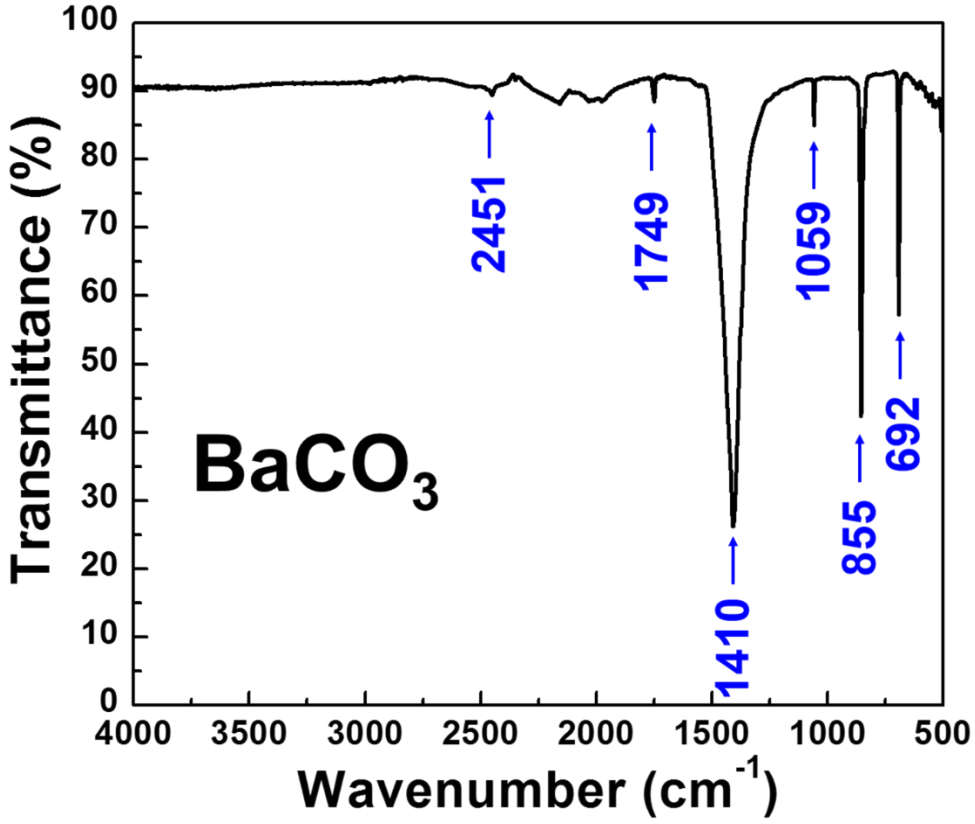

Fig. S9. FTIR pattern of $BaCO_3$ (Alfa Aesar, 99.95%). The pattern matches previous patterns reported in the literature.[S3]

Reference

(S3) Sreedhar, B.; Vani, C. S.; Devi, D. K.; Rao, M. V. B.; Rambabu, C. Shape Controlled Synthesis of Barium Carbonate Microclusters and Nanocrystallites Using Natural Polysachharide – Gum Acacia. *Am. J. Mater. Sci.* **2012**, *2*, 5–13.

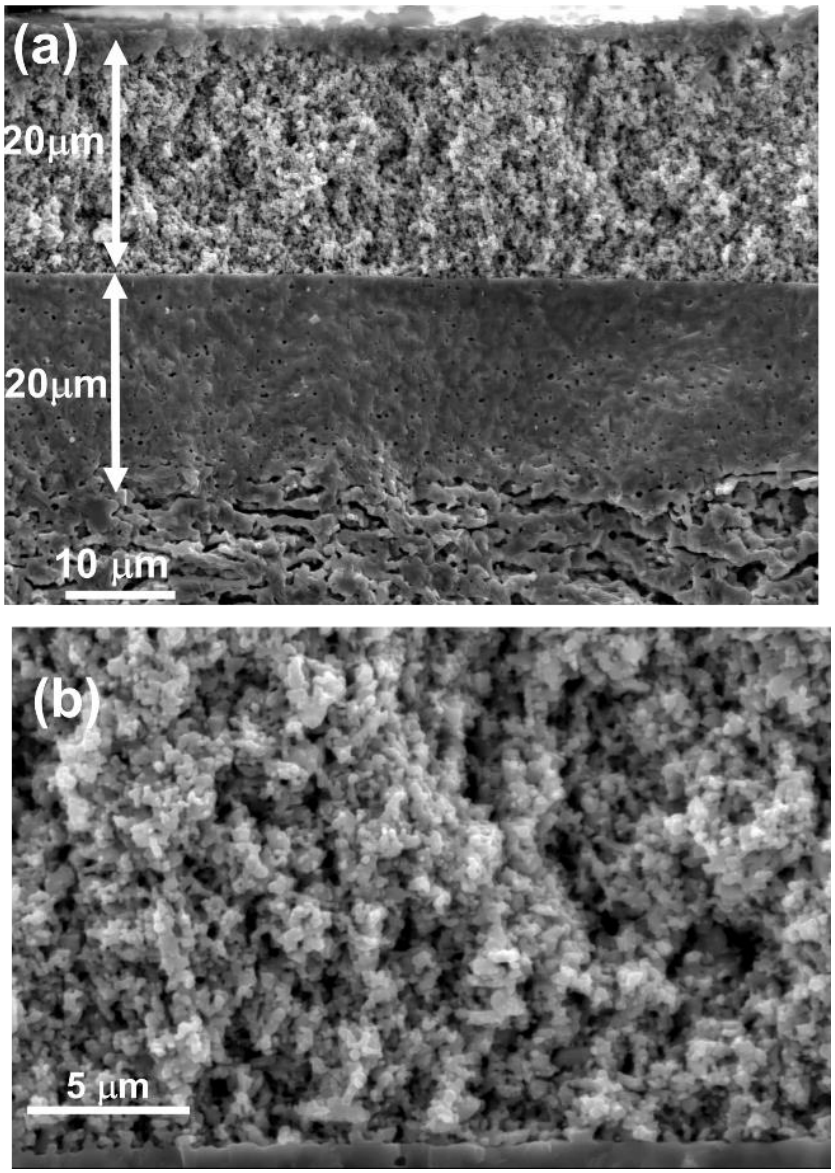

Fig. S10. Cross-sectional SEM images of (a) an anode-supported single cell and (b) a composite cathode layer before performance evaluation.